

LA-UR-

*Approved for public release;
distribution is unlimited.*

Title:

Author(s):

Submitted to:



Los Alamos National Laboratory, an affirmative action/equal opportunity employer, is operated by the University of California for the U.S. Department of Energy under contract W-7405-ENG-36. By acceptance of this article, the publisher recognizes that the U.S. Government retains a nonexclusive, royalty-free license to publish or reproduce the published form of this contribution, or to allow others to do so, for U.S. Government purposes. Los Alamos National Laboratory requests that the publisher identify this article as work performed under the auspices of the U.S. Department of Energy. Los Alamos National Laboratory strongly supports academic freedom and a researcher's right to publish; as an institution, however, the Laboratory does not endorse the viewpoint of a publication or guarantee its technical correctness.

Resonant Soft X-ray Contrast Variation Methods as Composition-Specific Probes of Thin Polymer Film Structure

*Cynthia F. Welch,^{*a} Rex P. Hjelm,^{*b} Joseph T. Mang,^c Marilyn E. Hawley,^a Debra A. Wroblewski,^a E.
Bruce Orler^a, & Jeffrey B. Kortright^d*

Materials Science & Technology Division, Los Alamos Neutron Science Center, and Dynamic
Experimentation Division, Los Alamos National Laboratory, Los Alamos, NM 87545, and Materials
Sciences Division, Lawrence Berkeley National Laboratory, Berkeley, CA 94720

cwelch@lanl.gov, hjelm@lanl.gov

**RECEIVED DATE (to be automatically inserted after your manuscript is accepted if required
according to the journal that you are submitting your paper to)**

^aMaterials Science & Technology Division, LANL

^bLos Alamos Neutron Science Center, LANL

^cDynamic Experimentation Division, LANL

^dMaterials Sciences Division, LBNL

We have developed complementary soft x-ray scattering and reflectometry techniques that allow for the morphological analysis of thin polymer films without resorting to chemical modification or isotopic

labeling. With these techniques, we achieve significant, x-ray energy-dependent contrast between carbon atoms in different chemical environments using soft x-ray resonance at the carbon edge. Because carbon-containing samples absorb strongly in this region, the scattering length density depends on both the real and imaginary parts of the atomic scattering factors. Using a model polymer film of poly(styrene-*b*-methyl methacrylate), we show that the soft x-ray reflectivity data is much more sensitive to these atomic scattering factors than the soft x-ray scattering data. Nevertheless, fits to both types of data yield useful morphological details on the polymer's lamellar structure that are consistent with each other and with literature values.

Introduction

Thin films of carbon-containing materials are found in a pervasive number of applications,¹⁻⁵ ranging from well-established industrial binders and coatings to novel biomedical and optoelectronic devices based on recent advances in nanotechnology. Phase separation through self-assembly gives these films the properties required by these applications; thus, determining the film structure and understanding its formation are key to unraveling the structure-property relationships. However, determining the morphology of thin, carbon-based films via traditional x-ray and neutron scattering techniques is often difficult due to weak contrast between phases and small scattering volumes. Consequently, standard scattering techniques often require either heavy atom, for x-rays, or deuterium labeling, for neutrons, to locate the various chemical constituents in the structure. Here we develop soft x-ray scattering and reflectometry techniques that allow us to analyze the morphology of thin polymer films whose phase-separated domains are distinguishable without resorting to chemical modification or isotopic labeling. With these techniques, we achieve significant, x-ray energy-dependent contrast between carbon atoms in different chemical environments using soft x-ray resonance at the carbon edge. We demonstrate the use of this contrast mechanism on the phase-separated structure of a model thin polymer film. While the realization of these methods represents a significant advance in our ability to probe the morphology

of thin polymer films, we expect that they will also find extensive use in the analysis of other thin, carbon-containing films often found in biological systems and new nanocomposite devices.

Soft x-rays encompass an energy range (250 – 2500 eV) that includes the K absorption edges of light elements (e.g., C, N, O, Si, P, S). The strong resonances in the atomic scattering factor, f , that occur near these edges result in large, energy-dependent variation in scattering amplitude near and across the absorption edge. The resonant energy for a given element (e.g., C) depends on its chemical environment (e.g., C=C vs. C=O), resulting in significant differences in $f(E)$ and an energy-dependent variation in scattering interferences, or contrast, between atoms of the same element in different chemical environments. This phenomenon is the basis for resonant x-ray scattering, a method of contrast variation⁶ that has been largely limited to examining the local structure around heavy elements with higher energy absorption edges in the hard x-ray region. The use of soft x-ray resonance has been of increasing interest for resolving structure in magnetic^{7, 8} and correlated electron systems.^{9, 10} In polymers, this contrast mechanism has proven useful in soft x-ray microscopy,¹¹ and, more recently, in soft x-ray reflectometry^{12, 13} (RSoXR) and scattering¹⁴⁻¹⁷ (RSoXS) of polymer films and nanoparticles. Otherwise, most applications of resonant x-ray scattering to polymers¹⁸⁻²¹ have heretofore been with hard x-rays. Like contrast variation techniques used in neutron scattering, which require labeling with deuterium, hard x-ray resonance scattering requires chemical labeling using substituted heavy elements.

Here, we report complementary RSoXS and RSoXR measurements that take advantage of soft x-ray resonance to generate energy-dependent contrast variation between carbon atoms of different chemical groups. This technique allows us to probe phase-separated domain structure and composition on the nano-scale in thin polymer films without any chemical labeling or other modifications. A preliminary report of part of this work was published in a recent proceedings of The American Chemical Society.¹⁶

Experimental

Materials. Films of the symmetric diblock copolymer poly(styrene-*b*-methyl methacrylate) (PS-PMMA, 42,000 g/mol, Polymer Source) were prepared by spin-coating a 40 mg/mL solution in toluene

onto clean glass or silicon substrates, annealing at 170°C under vacuum, and quenching to 20°C on a thick metal plate. To create free-standing films for transmission and scattering experiments, the films coated on the glass slides were floated onto water; this method was successful in creating uniform films with areas of at least 0.25 cm² and thicknesses of 100 – 300 nm. Free-standing films were mounted on aluminum squares with 5 mm x 2 mm slit or 2-mm diameter circular openings.

Measurements. Soft x-ray experiments were conducted at beam line 6.3.2 at the Advanced Light Source, Lawrence Berkeley National Laboratory. A 600-line/mm monochromator with ~0.15 eV resolution was used for all scattering and reflectometry measurements. Reflectometry experiments were performed with films in silicon substrates, whereas transmission and scattering measurements were conducted with free-standing films in transmission geometry, relative to the incident beam. Scattering data was collected using theta-energy scans and a Channeltron detector. To avoid radiation damage, each energy scan was done at a different location on the film. Transmission spectra and reflectivity data were collected with a wire (photodiode) detector.

Calculations. By normalizing the transmission spectra against sample thickness, density, and chemical composition, we obtained the imaginary or absorptive part of the atomic scattering factor for

carbon atoms in each polymer as a function of energy, $f_C''(E)$:
$$f_C''(E) = \frac{1}{x_C} \left[\frac{\mu(E)M}{2b_0N_A\lambda} - \sum_i x_i f_i''(E) \right],$$

where E is energy, μ is the mass absorption coefficient, M is the molecular weight, b_0 is the scattering length of a free electron, N_A is Avogadro's number, λ is the wavelength, x_i is the number of atoms of type i , the subscript C refers to carbon atoms, and the summation is over all atoms. The experimental data was then scaled to the standard carbon absorption edge and spliced into the tabulated values of f_C'' .²² The real part of the atomic scattering factor $f_C'(E)$ was calculated via the Kramers-Kronig transformation of $f_C''(E)$, using the method of Hoyt et al.²³ By combining these measured values of f_C' and f_C'' with tabulated atomic scattering factors²² for all other atoms in each polymer, we calculated the scattering length densities (ρ) and the complex refractive index components (δ and β) of the two

polymers as a function of energy. The energy-dependent scattering length density is calculated as $\rho(E) = \Sigma b(E)_i/V$, where V is volume and the scattering length $b(E) = b_0(Z + f_i'(E) + if_i''(E))$, where Z is the atomic number. The averaged squared contrast for a two-phase system is given by the Debye expression $\overline{\Delta\rho^2} = \Phi(1 - \Phi)(\rho_{PS} - \rho_{PMMA})^2$, where Φ is the volume fraction of one of the phases. The complex index of refraction, $n(E) = 1 - \delta(E) - i\beta(E) = 1 - \lambda^2\rho(E)/2\pi$, is related to the atomic scattering factors: $\delta(E) = \frac{\rho_m N_A b_0 \lambda^2}{2\pi M} \sum n_i f(E)_i'$ and $\beta(E) = \frac{\rho_m N_A b_0 \lambda^2}{2\pi M} \sum n_i f(E)_i''$, where ρ_m is the mass density.

The low- Q scattering from the free-standing thin films was modeled as a lamellar phase of stacked, rectangular sheets with sharp phase boundaries, $I(Q) \propto \left\langle \left| F(Q_x, Q_y, Q_z) S(Q_z) \right|^2 \right\rangle$, where $F(Q_x, Q_y, Q_z)$ is the form factor of a layer and $S(Q_z)$ is the structure factor along the z -axis; the brackets indicate an average over the distribution of orientations of the lamellae relative to the incident beam, which was taken to be in either of two states: parallel or perpendicular ($90^\circ \pm 5^\circ$) to the plane of the film. Although the lamellae were expected to align primarily parallel to the plane of the film, or perpendicular to the incident x-ray beam in transmission scattering geometry, the presence of some lamellae aligned perpendicular ($90^\circ \pm 5^\circ$) to the plane of the film had to be included in the model to account for the peak observed in the low- Q scatter from the free-standing films (see Results & Discussion, Figure 2). The scattering length density was assumed to vary only along the z -axis of the lamellar stacks. Thus, the form factor along the x - and y -axes was given by $F_i(Q_i) = L_i \text{sinc}\left(\frac{Q_i L_i}{2}\right)$, where $i = x$ or y , L_i is the sheet dimension in a given direction and $\text{sinc}(x) = \sin(x)/x$. Along the direction parallel to the layer normal (the z -axis), the form factor was expressed as

$$F_z(Q_z) = \rho_{PMMA} L_z \text{sinc}\left(\frac{Q_z L_z}{2}\right) + \Delta\rho_{PS-PMMA} L_{PS} \text{sinc}\left(\frac{Q_z L_{PS}}{2}\right),$$

where $L_z = 1.92 L_{PS}$ and the scattering length densities are complex quantities computed as shown in Figure 1. The structure factor along z was that

for a finite, perfect 1-D lattice, $S(Q_z) = \frac{\sin(\frac{NQ_z d_z}{2})}{N \sin(\frac{Q_z d_z}{2})}$, where N is the number of layers and $d_z = L_z$.

Results and Discussion

Near the carbon absorption edge (~ 284 eV), transmission spectra (e.g., Figure 1a) reveal the excitation energies required to promote core (1s) electrons of carbon atoms into anti-bonding π^* and σ^* orbitals; these spectroscopic fingerprints, commonly called near edge x-ray absorption fine structure (NEXAFS), are highly dependent on the bonding chemistry of the carbon atoms involved.²⁴ We capitalize on these spectroscopic differences to generate contrast between different types of carbon atoms in RSoXS and RSoXR experiments that enable us to investigate structural features at the nanometer level (1 – 50 nm). To develop these capabilities for complex phase-separating systems, we examined poly(styrene-*b*-methyl methacrylate) (PS-PMMA) diblock copolymers, whose phase behavior is well-understood.

Differences in the soft x-ray transmission spectra of the homopolymers polystyrene (PS) and poly(methyl methacrylate) (PMMA) imply differences in the atomic scattering factors of these two polymers (Figure 1a, b). The imaginary part of the atomic scattering factor f_C'' is a measure of the absorption by carbon atoms in each polymer, while the real part f_C' is a measure of the dispersion. The aromatic carbon atoms in PS absorb strongly at ~ 285 eV; in contrast, the carbonyl ester carbon in PMMA has an intense absorption at ~ 288 eV.²⁵ From the data in Figure 1b, we calculated the squared difference in scattering length densities ($= (\rho_{PS} - \rho_{PMMA})^2$) of the two polymers as a function of energy (Figure 1c). This result is proportional to the energy-dependent scattering intensity from completely segregated domains of PS and PMMA. This strong contrast results directly from differences in the chemical make-up of the two polymers, with the sharp peaks at ~ 285 and ~ 288 eV due to PS aromatic carbon absorption and PMMA ester carbonyl absorption, respectively. These core to π^* transitions provide a stronger contrast than the core to σ^* transitions in the energy region above 290 eV.

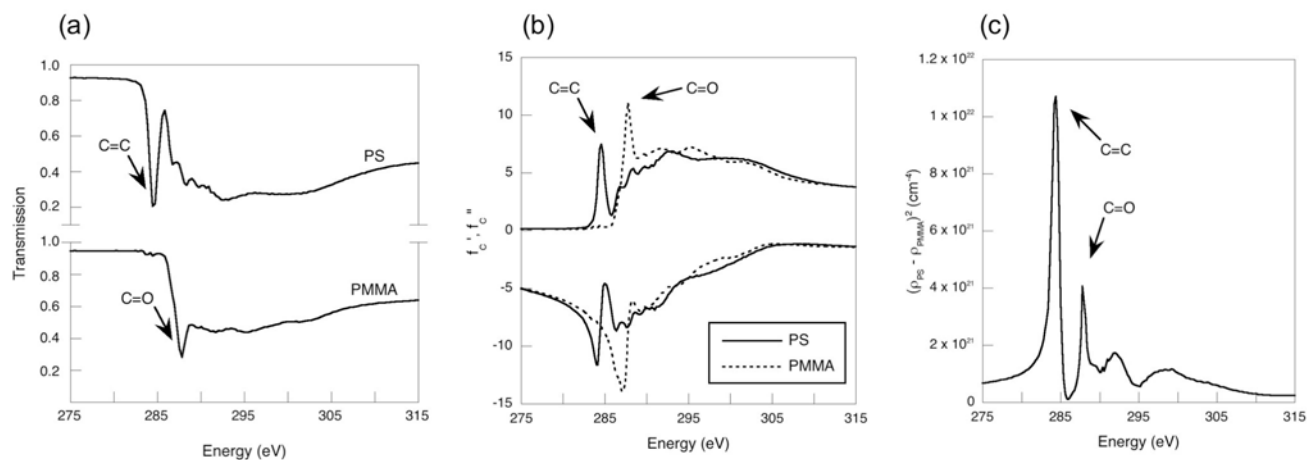


Figure 1. Soft x-ray (a) transmission spectra, (b) atomic scattering factors, and (c) the contrast from calculated scattering length densities for PS and PMMA homopolymers.

We examined the low- Q scattering behavior of a thin, free-standing film of a symmetric PS-PMMA diblock copolymer film in transmission mode, as shown in Figure 2. We observed a sharp peak at $Q = 4\pi(\sin\theta)/\lambda \approx 0.023 \text{ \AA}^{-1}$, which is consistent with a lamellar morphology with a period of $\sim 28 \text{ nm}$. Such a structure agrees with expectations based on literature data for other symmetric PS-PMMA diblock copolymers²⁶⁻²⁹ and with a self-consistent field (SCF) calculation for this diblock.³⁰

Because the contrast between PS and PMMA is a strong function of incident soft x-ray energy (as shown in Figure 1c), the peak heights in Figure 2 vary strongly as a function of energy. The presence of the peak indicates that some of the lamellae are oriented perpendicular to the plane of the thin film. This perpendicular orientation could exist as defects in the interior of the film or on the film's surface, i.e., around the circumference of lamellae islands^{27, 28} that we have observed by AFM (data not shown) on similarly prepared samples. To fit this data, we modeled the polymer film as stacked lamellar sheets, with the majority oriented parallel to the plane of the film and a small fraction in the perpendicular ($90^\circ \pm 5^\circ$) direction. The difference in scattering length densities between PS and PMMA at each incident x-ray energy was taken from the $\Delta\rho^2(E)$ curve shown in Figure 1c, thereby assuming a strong segregation of the PS and PMMA layers. The ratio between PS and PMMA lamellar widths was taken from the

extensive literature²⁶⁻²⁹ for other symmetric PS-PMMA diblock copolymers, i.e., $d_{\text{PMMA}} = 0.92d_{\text{PS}}$. The morphological parameters obtained from the fits at each incident x-ray energy were the lamellar bilayer period d ($= 28.2 \pm 0.6$ nm), the number of bilayers in the stacked sheet N ($= 7$), the length L_x ($= 55 \pm 15$ nm) and width L_y ($= 68 \pm 11$ nm) of the stacked sheet, respectively, and the fraction of lamellae aligned perpendicular to the plane of the film F_{out} (0.085 ± 0.052). This lamellar model fits the data well, as shown by the solid lines in Figure 2, and yields reasonable values of the fit parameters for this polymer.

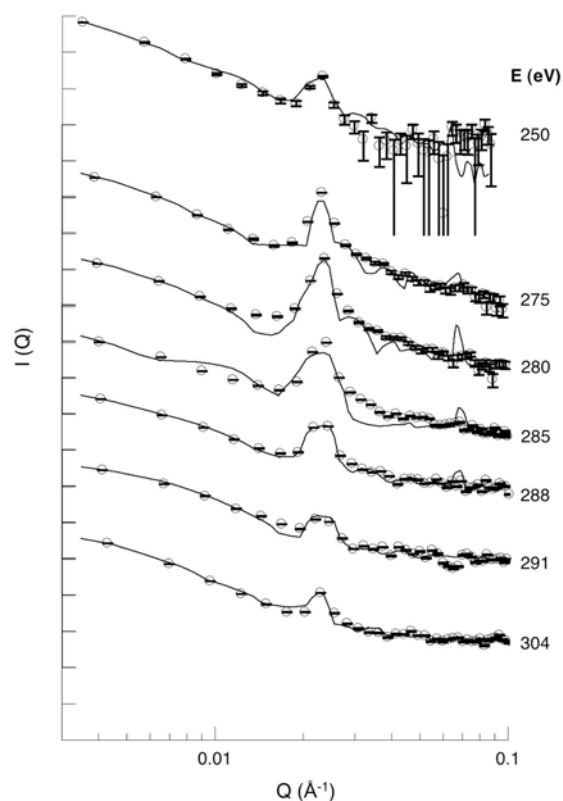


Figure 2. Low-Q soft x-ray scattering data (open circles) from a free-standing PS-PMMA, symmetric diblock copolymer film and model fits (solid lines) at seven different soft x-ray incident energies. The ordinate is log intensity in arbitrary units with decades indicated on the axis. The data at various energies are shifted downward by decades relative to the lowest energy (250 eV): 275 eV, -5; 280 eV, -7; 285 eV, -10; 288 eV, -12; 291 eV, -14; 304 eV, -16. The scattering length densities for the PS and PMMA domains were calculated from soft x-ray transmission spectra of the homopolymers (Figure 1).

Figures 3a and 3b show reflectivity data and initial model fits for two PS-PMMA films (200-nm and 70-nm thick, respectively) on silicon substrates. A multilayer model³¹ that uses the complex indices of refraction ($n = 1 - \delta - i\beta$) of each layer was used to fit the data. As with the fits to the scattering data, we fixed some parameters: $d_{\text{PMMA}} = 0.92d_{\text{PS}}$, a PS half-layer at the surface and a PMMA half-layer at the interface with the silicon substrate. For the initial fits shown in Figure 3, the refractive index components δ and β for the individual PS and PMMA layers were calculated directly from the soft x-ray transmission spectra and atomic scattering factors of the respective homopolymers (Figure 1). Below the absorption edge, this initial model fits the data well to give structures in agreement with expectations for both films. Three parameters come from these fits to the data: d (26.6 and 27.7 nm), N (7.5 and 2.5), and σ (1.8 nm), where σ is the interfacial roughness / diffuseness with a sinusoidal interface profile. This same structure is used to calculate the model reflectivity at and above the absorption edge, but here discrepancies between the model and data clearly exist. Although the general shape of the curve is matched, the model under-predicts the magnitude of the reflectivity at each energy. Further, the model curves are generally shifted to lower Q_z with respect to the data, which causes the model fits to miss the location of the Bragg peaks.

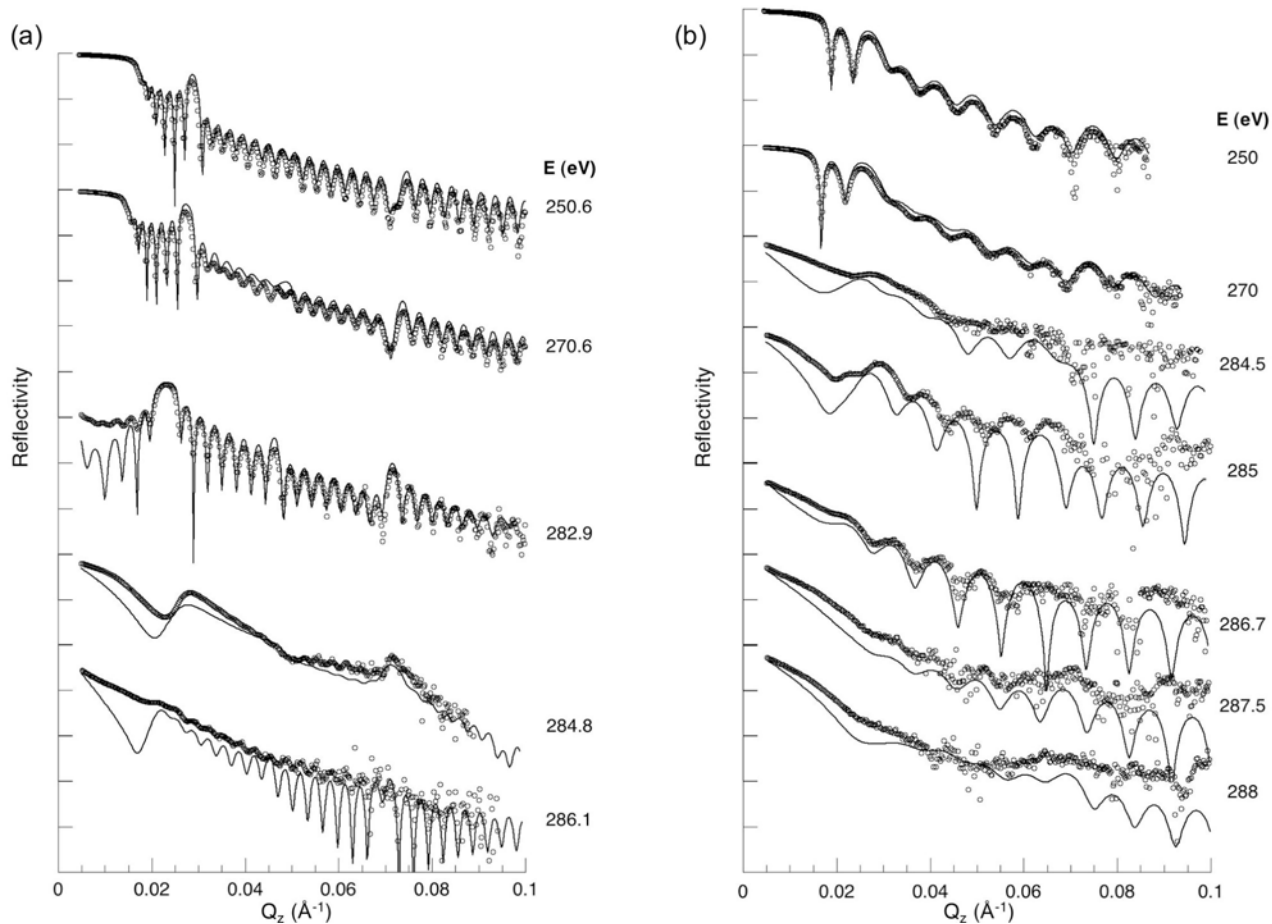


Figure 3. Soft x-ray reflectivity data (open circles) and initial model fits (solid lines) for two PS-PMMA diblock copolymer films. The ordinate is log scale with decades indicated on the axis, with the maximum tick mark at $R = 1$. (a) 200-nm thick: $d = 26.6$ nm, $N = 7.5$, $\sigma = 1.8$ nm; data are shifted downward by decades relative to the lowest energy (250.6 eV): 270.6 eV, -3; 282.9 eV, -7; 284.8 eV, -11; 286.1 eV, -13. (b) 70-nm thick: $d = 27.7$ nm, $N = 2.5$, $\sigma = 1.8$ nm; data are shifted downward by decades relative to the lowest energy (250 eV): 270 eV, -3; 284.5 eV, -5; 285 eV, -7; 286.7 eV, -10; 287.5 eV, -12; 288 eV, -14. The refractive index components δ and β were calculated directly from the soft x-ray transmission spectra and atomic scattering factors of the respective homopolymers (Figure 1).

By holding d , N , and σ fixed at the values given above, we obtained better fits if δ and β for PS and PMMA were allowed to vary from their calculated values. The fits shown in Figures 4a and 4b were obtained from this fitting procedure (i.e., allowing δ and β to vary) for data at energies that span the

range below and above the carbon absorption edge, and Figures 5a and 5b compare the fit values of δ and β to the calculated values. While no specific attempt to ensure self-consistency of the fitted δ and β values was made, the fitted values deviate from the original values in a manner consistent with expectations from the Kramers-Kronig dispersion relation. Below the absorption edge, the fit values for the refractive index components vary only slightly from the calculated values, but good fits to data above the absorption edge required larger variations in δ and β . These δ - and β -fit values suggest a higher contrast between PS and PMMA than that calculated from the transmission spectra (Figure 1c). Interestingly, if these δ - and β -fit values are used to calculate the contrast terms in modeling the scattering data of Figure 2, equally good fits (see Figure 6) with similar results are obtained: $d = 28.1 \pm 0.7$ nm, $N = 7$, $L_x = 56 \pm 14$ nm, $L_y = 73 \pm 15$ nm, and $F_{out} = 0.035 \pm 0.021$. This result suggests that the reflectivity measurements are much more sensitive to small changes in the atomic scattering factors, at least for the PS-PMMA symmetric diblock copolymer studied here.

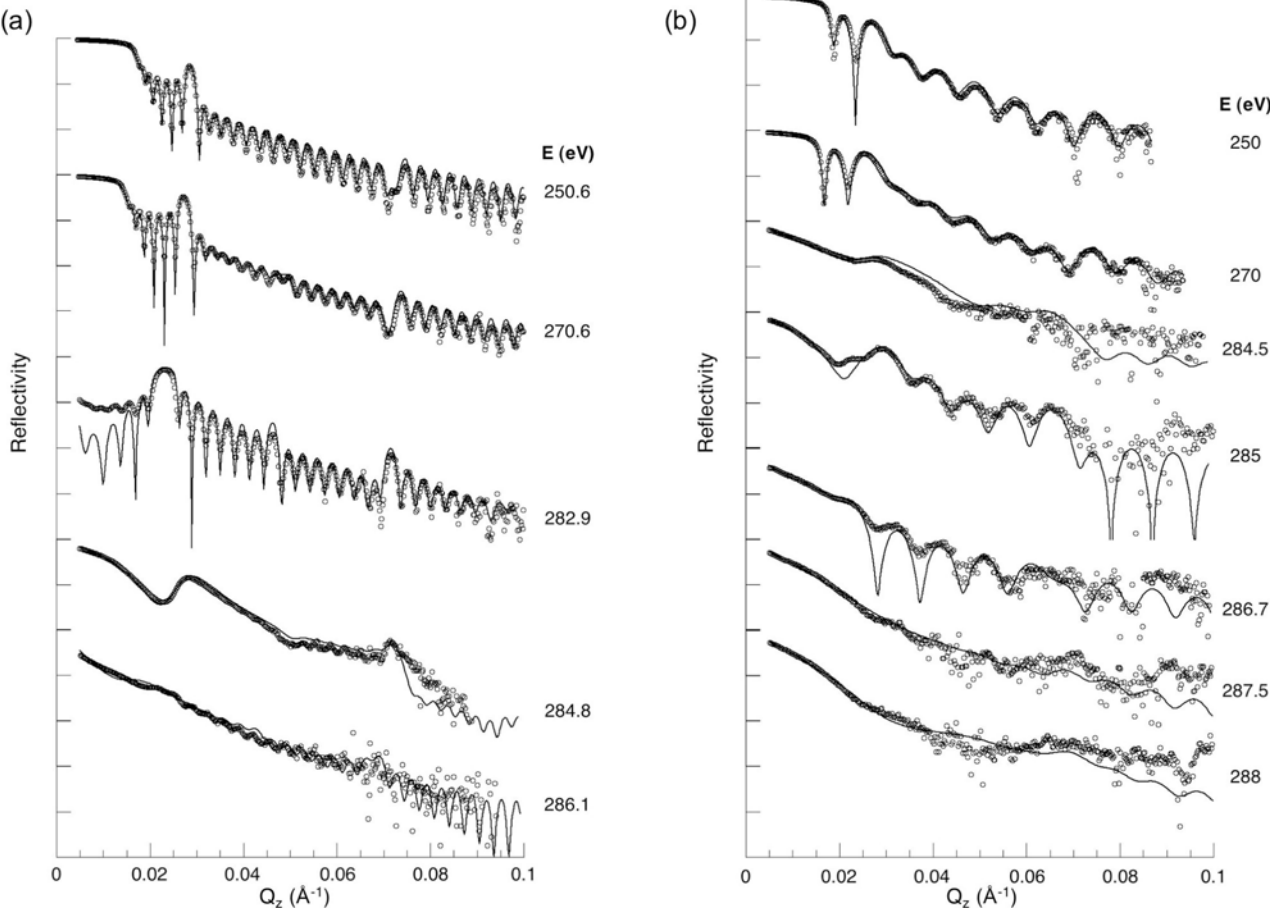


Figure 4. Soft x-ray reflectivity data (open circles) and refined model fits (solid lines) for the two PS-PMMA diblock copolymer films of Figure 3. (a) and (b) are as described in Figure 3, but with refractive index components δ and β used as fit parameters.

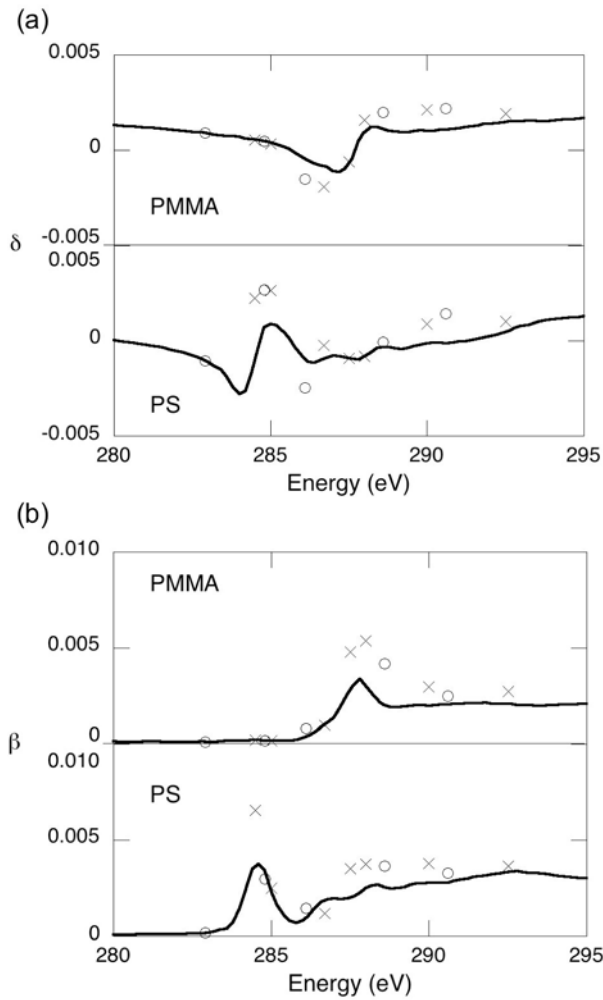


Figure 5. Reflectivity fit values (symbols) of (a) δ and (b) β compared to those calculated from transmission measurements (solid lines), as a function of soft x-ray incident energy. Open circles represent fit values obtained for data of the 200-nm PS-PMMA film (of Figure 4a), while the “x” symbols are from the 70-nm film (of Figure 4b).

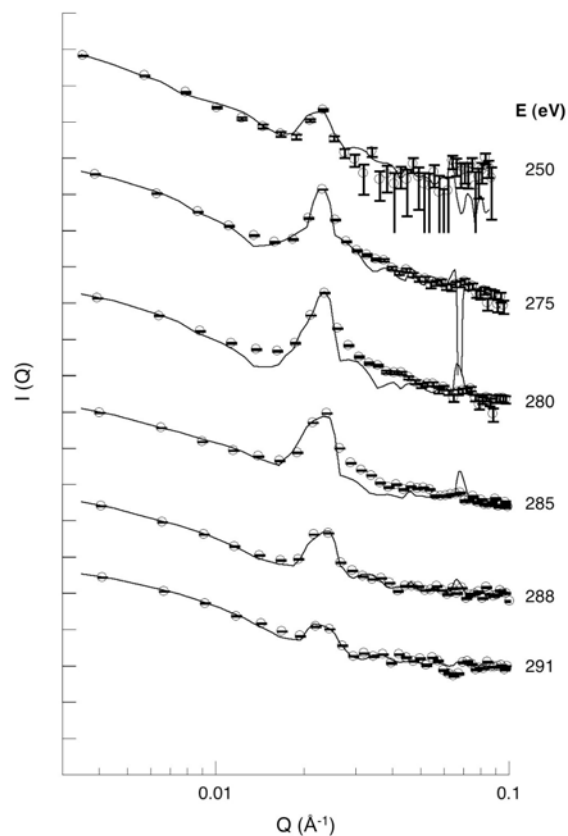


Figure 6. Low-Q soft x-ray scattering data (open circles) and fits (solid lines) for the PS-PMMA free-standing film of Figure 2. Here, the scattering length densities for the PS and PMMA domains were taken from the refined fits to the soft x-ray reflectivity data, in which δ and β were used as fit parameters.

The small discrepancies between the computed and fitted refractive index components most likely result from differences in orientation of the styrene and methacrylate moieties in the diblock copolymer as compared to the homopolymers. The intensity of the absorption resonances (shown for the homopolymers in Figure 1) depends on the angle between the polarized electric field vector of the x-rays and the orientation of the valence orbitals involved in the resonance absorption (e.g., the π orbitals of the PS phenyl or the PMMA ester).²⁴ Any differences in the average orientation of valence orbitals in the homopolymers vs. the diblock copolymer would result in differences in absorption intensities and,

likewise, in the refractive index components. Other possible explanations include those put forth by Wang et al.,¹² who noted similar discrepancies between computed and fitted δ and β values, and differences in the spectral contamination of the beam at the time of the homopolymer measurements vs. the time of the copolymer measurements.

Conclusion

The soft x-ray scattering and reflectivity results from the PS-PMMA diblock copolymer use the natural contrast between different types of carbon atoms in the soft x-ray energy range to obtain the morphology of thin polymer films. Our complementary RSoXS and RSoXR data demonstrate the sensitivity of these techniques. With RSoXS, we could extract morphological information on lamellar bilayers when the fraction of lamellae oriented perpendicular to the plane of the film was quite small. Further, the RSoXR results suggest a contrast that is not only dependent on the chemical bond types, but also may depend on the orientation of those bonds. This contrast mechanism provides a path forward to solving the phase-separated thin film structure of more complicated systems, such as segmented block copolymers that would require chemical modification for examination with traditional x-ray and neutron scattering techniques.^{16, 32} These advances in thin film characterization will enhance our understanding of their structure-property relationships and our subsequent ability to tailor thin film properties for a variety of applications. Soft x-rays hold great promise as a chemical bond-specific probe of compositional heterogeneity in thin films, with concomitant benefits in applying contrast variation techniques to solve the structure and composition of materials without the complications associated with chemical modification or isotopic labeling.

Acknowledgements. Soft x-ray measurements were conducted at the Advanced Light Source, which is supported by the Director, Office of Science, Office of Basic Energy Sciences, of the U.S. Department of Energy under Contract No. DE-AC02-05CH11231. Funding was provided by the U.S. Department of Energy at Los Alamos National Laboratory, operated by the University of California

References

1. Fasolka, M. J.; Mayes, A. M. *Annu. Rev. Mater. Res.* **2001**, *31*, 323-355.
2. Hammond, P. T. *Advanced Materials* **2004**, *16*, 1271-1293.
3. Piqué, A.; Auyeung, R. C. Y.; Stepnowski, J. L.; Weir, D. W.; Arnold, C. B.; McGill, R. A.; Chrisey, D. B. *Surface & Coatings Technology* **2003**, *163-164*, 293-299.
4. Prasad, P. N. *Current Opinion in Solid State and Materials Science* **2004**, *8*, 11-19.
5. Tien, H. T.; Ottova, A. L. *Journal of Membrane Science* **2001**, *189*, 83-117.
6. Schurtenberger, P., Contrast and contrast variation in neutron, x-ray and light scattering. In *Neutrons, X-rays and Light: Scattering Methods Applied to Soft Condensed Matter*, Lindner, P.; Zemb, T., Eds. Elsevier: Amsterdam, 2002; pp 145-170.
7. Dürr, H. A.; Dudzik, E.; Dhesi, S. S.; Goedkoop, J. B.; Laan, G. v. d.; Belakhovsky, M.; Mocuta, C.; Marty, A.; Samson, Y. *Science* **1999**, *284*, 2166-2168.
8. Kortright, J. B.; Kim, S.-K.; Denbeaux, G. P.; Zeltzer, G.; Takano, K.; Fullerton, E. E. *Physical Review B: Condensed Matter* **2001**, *64*, 092401.
9. Abbamonte, P.; Blumberg, G.; Rusydi, A.; Gozar, A.; Evans, P. G.; Siegrist, T.; Venema, L.; Eisaki, H.; Isaacs, E. D.; Sawatzky, G. A. *Nature* **2004**, *431*, 1078-1081.
10. Wilkins, S. B.; Spencer, P. D.; Hatton, P. D.; Collins, S. P.; Roper, M. D.; Prabhakaran, D.; Boothroyd, A. T. *Physical Review Letters* **2003**, *91*, 167205.
11. Ade, H.; Zhang, X.; Cameron, S.; Costello, C.; Kirz, J.; Williams, S. *Science* **1992**, *258*, 972-975.
12. Wang, C.; Araki, T.; Ade, H. *Applied Physics Letters* **2005**, *87*, 214109.
13. Wang, C.; Araki, T.; Watts, B.; Harton, S.; Koga, T.; Basu, S.; Ade, H. *J. Vac. Sci. Technol. A* **2007**, *25*, 575-586.
14. Araki, T.; Ade, H.; Stubbs, J. M.; Sundberg, D. C.; Mitchell, G. E.; Kortright, J. B.; Kilcoyne, A. L. D. *Applied Physics Letters* **2006**, *89*, 124106.
15. Mitchell, G. E.; Landes, B. G.; Lyons, J.; Kern, B. J.; Devon, M. J.; Koprinarov, I.; Gullikson, E. M.; Kortright, J. B. *Applied Physics Letters* **2006**, *89*, 044101.
16. Welch, C. F.; Hjelm, R. P.; Mang, J. T.; Wroblewski, D. A.; Orler, E. B.; Hawley, M. E.; Kortright, J. B. *Polymeric Materials Science and Engineering* **2005**, *93*, 288-290.
17. Virgili, J. M.; Tao, Y.; Kortright, J. B.; Balsara, N. P.; Segalman, R. A. *Macromolecules* **2007**, *40*, 2092-2099.
18. Ding, Y. S.; Hubbard, S. R.; Hodgson, K. O.; Register, R. A.; Cooper, S. L. *Macromolecules* **1988**, *21*, 1698-1703.
19. Fishburn, J. R.; Barton, S. W. *Macromolecules* **1995**, *28*, 1903-1911.
20. Sabbagh, I.; Delsanti, M.; Lesieur, P. *Eur. Phys. J. B* **1999**, *12*, 253-260.
21. Stuhmann, H. B. *Advances in Polymer Science* **1985**, *67*, 123-163.
22. Henke, B. L.; Gullikson, E. M.; Davis, J. C. *Atomic Data and Nuclear Data Tables* **1993**, *54*, 181-342.
23. Hoyt, J. J.; de Fontaine, D.; Warburton, W. K. *Journal of Applied Crystallography* **1984**, *17*, 344-351.
24. Stöhr, J., *NEXAFS Spectroscopy*. Springer-Verlag: Berlin, 1992; Vol. 25.
25. Dhez, O.; Ade, H.; Urquhart, S. G. *Journal of Electron Spectroscopy and related Phenomena* **2003**, *128*, 85-96.
26. Anastasiadis, S. H.; Russell, T. P.; Satija, S. K.; Majkrzak, C. F. *Journal of Chemical Physics* **1990**, *92*, 5677-5691.
27. Mayes, A. M.; Russell, T. P.; Bassereau, P.; Baker, S. M.; Smith, G. S. *Macromolecules* **1994**,

27, 749-755.

28. Russell, T. P.; Coulon, G.; Deline, V. R.; Miller, D. C. *Macromolecules* **1989**, *22*, 4600-4606.

29. Russell, T. P.; Mayes, A. M.; Bassereau, P. *Physica A: Statistical and Theoretical Physics* **1993**, *200*, 713-721.

30. Welch, C. F.; Welch, P. M.; Hjelm, R. P. *in preparation* **2008**.

31. Windt, D. L. *Computers in Physics* **1998**, *12*, 360-370.

32. Welch, C. F.; Hjelm, R. P.; Mang, J. T.; Hawley, M. E.; Wroblewski, D. A.; Orler, E. B.; Kortright, J. B. *in preparation*.

For Table of Contents Use Only

Manuscript Title: Resonant Soft X-ray Contrast Variation Methods as Composition-Specific Probes of Thin Polymer Film Structure

Authors: Cynthia F. Welch, Rex P. Hjelm, Joseph T. Mang, Marilyn E. Hawley, Debra A. Wroblewski, E. Bruce Orler, Jeffrey B. Kortright

